Carrier recombination flux in bulk heterojunction polymer:fullerene solar cells: Effect of energy disorder on ideality factor

Germà Garcia-Belmonte *

Photovoltaic and Optoelectronic Devices Group, Departament de Física, Universitat Jaume I, ES-12071 Castelló, Spain

A B S T R A C T

Energy disorder reduces the achievable open-circuit voltage in organic bulk-heterojunction solar cells. Here the effect of disorder on charge carrier recombination flux is numerically modeled. The recombination current follows an exponential dependence on voltage (Fermi level splitting) parameterized by β (inverse of the diode ideality factor), which reduces the power conversion efficiency through lower fill factors. β-Parameter approaches unity (Boltzmann approximation) at room temperature only in the case of weak disorder ($\sigma \approx 50$ meV). For larger disorder values ($\sigma \geqslant 100$ meV) usually encountered in real devices, a huge reduction in β (open-circuit voltage, and fill factor) is predicted following a relationship as $\beta \propto \ln \sigma^{-1}$.

© 2012 Elsevier Ltd. All rights reserved.

1. Introduction

Organic photovoltaic technology allows reducing the production costs of solar energy. A considerable effort has led very recently to achieve power conversion efficiencies near 10% in the case of bulk-heterojunction solar cell structures [1]. Although several limiting factors have been studied, and their detrimental effects quantified [2], further improvements need for detailed understanding of specific phenomena. Among others, energy disorder originated by either inherent complex structure, or polarization effects in organic solid films has been recently identified as a primary factor leading to reduction in open-circuit voltage V_{oc} [3–5]. Apart from influencing photovoltage, distributions of energy states have been identified as affecting charge carrier recombination kinetics through different charge transfer routes. Energetic tails of trapping states entering the effective gap of active materials has been proposed to affect the recombination rate by modulating the participation of mobile carriers into the recombination process [6–9]. Disorder energetic effects producing electronic density-of-states (DOS) were identified by means of subbandgap external quantum efficiency signals [10], and incorporated to device modeling [11] to analyze carrier recombination dynamics from transient photocurrent and photovoltage experiments [12].

A fruitful way to explore carrier recombination is by monitoring the open-circuit variation with irradiation intensity and temperature. Most models devised to simulate electrical response of organic solar cell are drawn upon regarding charge density as following the Boltzmann statistics [9,13,14]. In accordance with this approach a useful relation is expressed as

$$qV_{oc} = E_g - k_B T \ln \left(\frac{N_{LUMO} N_{HOMO}}{np} \right) \qquad (1)$$

Here $E_g = E_{LUMO}(A) - E_{HOMO}(D)$ corresponds to the effective energy gap. N_{LUMO}, and N_{HOMO} are the acceptor lowest-unoccupied molecular orbital (LUMO), and donor highest-occupied molecular orbital (HOMO) density-of-states, respectively. n (p) stands for the electron (hole) concentration. $k_B T$ is the thermal energy, and q the elementary charge. Eq. (1) can be used to derive a general dependence of V_{oc} on the irradiation intensity [14,15]. This was proposed by assuming that in the steady state under continuous irradiation, the effective photogeneration flux G equals the recombination flux R because no direct current is allowed to flow in open-circuit conditions, i.e. $R = G$ (or equivalently $j_{rec} = j_{ph}$ in terms of recombination current and photocurrent). The recombination flux is usually written as obeying a bimolecular law $R = knp$ (being k the recombination coefficient). Therefore V_{oc} depends on light intensity, which is proportional to G, following $V_{oc} \propto k_B T/q \ln G$ as derived from Eq. (1) [15]. The slope in the relationship $V_{oc} \propto \ln G$ equaling $k_B T/q$ has been reported in some cases, signaling a bimolecular-like recombination process with a charge density-independent k [14,15].

* Tel.: +34 964 387548; fax: +34 964 729218.
  E-mail address: garciag@fca.uji.es

In other cases larger slopes around $k_BT/\beta q$ with $\beta = 0.75$ have been observed in the experimental relationship $V_{oc} \propto \ln G$, and a change in the recombination mechanisms has been proposed to account for. Instead of a purely bimolecular recombination process, a trap-assisted recombination was employed in terms of the Shockley–Read–Hall (SRH) mechanism [16,17]. From that approach it is derived that the slope in the relation $V_{oc} \propto \ln G$ is a fingerprint of the particular recombination process governing the solar cell performance. Knowledge about the physical mechanisms influencing β-parameter is then of primary importance to improve organic photovoltaic devices.

However if the occupancy deviates from the simpler Boltzmann statistics because of the existence of density-of-states (DOS) distributions in the transport levels or tail states penetrating the band gap [18,19], able to capture free carriers, the determination of V_{oc} is only feasible by numerical calculation based on the more general expression $qV_{oc} = E_{Fn} - E_{Fp}$, written in terms of the separate carrier Fermi levels. In such cases a useful strategy to evaluate the output V_{oc} has been the determination of carrier concentration resulting from the kinetic balance between photogeneration and recombination rates [3]. Because this approach does not constrain the DOS occupancy to obey the Boltzmann function, the origin of the $V_{oc} \propto \ln G$ slope deviation from k_BT/q is not necessarily linked to a change in the recombination mechanism. We will next demonstrate that the slope of the relation $V_{oc} \propto \ln G$ is in fact determined by the energy disorder exhibited by electron (acceptor) and holes (donor) states. Typical values for the energy disorder of the DOS (~100 meV) [20,21] suffices to explain the observed slope values larger than k_BT/q. Moreover we will next show how expressions like Eq. (1) are limiting cases only valid for weak (<50 meV) disorder.

We will also state that the β-parameter ($\beta \leqslant 1$) in the relationship $V_{oc} \propto k_BT/\beta q \ln G$ corresponds to the inverse of the diode ideality factor of the current density–voltage characteristics j–V, dominated by the carrier recombination current as [22]

$$j_{rec} = j_0 \exp\left(\beta \frac{V}{k_BT/q}\right) \qquad (2)$$

where j_0 stands for the reverse, dark current. As pointed out in previous works β, along with transport properties determining the series resistance, is one of the parameters determining the fill-factor of the j–V characteristics which directly affects the power conversion efficiency η [23,24].

2. Results and discussion

In terms of the experimental curves exhibited by bulk-heterojunction solar cells under illumination, the response can be well fitted by means of an expression as

$$j = j_0\left[\exp\left(\beta \frac{V}{k_BT/q}\right) - 1\right] - j_{ph} \qquad (3)$$

Very recently we have addressed the phenomenology of recombination expressed in Eq. (2) by looking at the recombination current derivative (so-called recombination resistance introduced below) using impedance spectroscopy measurements [25]. Eq. (3) describes well empirical responses when $V = V_F$ represents the splitting of the electron and hole Fermi levels [22]. We have observed that for poly(3-hexylthiophene) (P3HT) and [6,6]-phenyl C_{61}-butyric acid methyl ester (PCBM) solar cells recombination and photogeneration currents are separated terms, i.e. recombination current results independent of the illumination level, and photocurrent is voltage-independent [25].

In this study polymer solar cells were fabricated using a standard sandwich structure of ITO/PEDOT:PSS/P3HT:PCBM/Ca, and 9 mm^2 of active area. Pre-cleaned ITO coated glass substrates (10 Ω/sq) were treated in a UV-O$_3$ chamber for 5 min followed by the deposition

of PEDOT:PSS by spin coating in air at 5500 rpm for 30 s, film thickness of ~35 nm. The substrates were heated at 120 °C for 10 min to remove traces of water and were transferred to a glove box equipped with a thermal evaporator. The P3HT:PCBM layer was deposited at speeds of 1200 rpm (thickness was about 110 nm) for 20 s followed by a slow drying process in a petry dish to provide a dry film. At this point, all samples were thermally annealed at 130 °C for 10 min to provide an adequate morphology and to promote oxygen desorption. Evaporation of the upper contact was carried out at a base pressure of 3×10^{-6} mbar with Ca/Ag (5/100 nm). Devices were encapsulated with a photoresin and a glass microscopy slide followed by exposure under UV light. Samples were then taken out of the glove box for device characterization.

The kinetics of the recombination current j_{rec} is accessible by measuring the impedance response of the solar cell in open-circuit conditions [26]. Impedance spectroscopy is a small-amplitude electrical technique especially suited to extract ac parameters that complements common dc analysis as j–V curves. In this study j–V characteristics and impedance spectroscopy measurements were carried out by varying irradiation intensity (1.5G illumination source 1000 W m^{-2}) using an Abet Sun 2000 Solar Simulator. The light intensity was adjusted with a calibrated Si solar cell. Impedance spectroscopy measurements were performed with Autolab PGSTAT-30 equipped with a frequency analyzer module, and was recorded by applying a small voltage perturbation (20 mV rms). Measurements were carried out at different light intensity in open-circuit conditions sweeping frequencies from 1 MHz down to 100 Hz. The light intensity was measured using an optical power meter 70,310 from Oriel Instruments where a Si photodiode was used to calibrate the system.

The impedance spectra are characterized by a major RC arc plus additional minor features at high frequency. The low frequency arc is attributed to the processes of carrier recombination (resistance R_{rec}) and charge storage (chemical capacitance C_μ) in the photoactive blend [27]. The measured recombination resistance is in fact the derivative of the recombination flux as

$$R_{rec} = \frac{1}{L}\left(\frac{dj_{rec}}{dV_{oc}}\right)^{-1} \qquad (4)$$
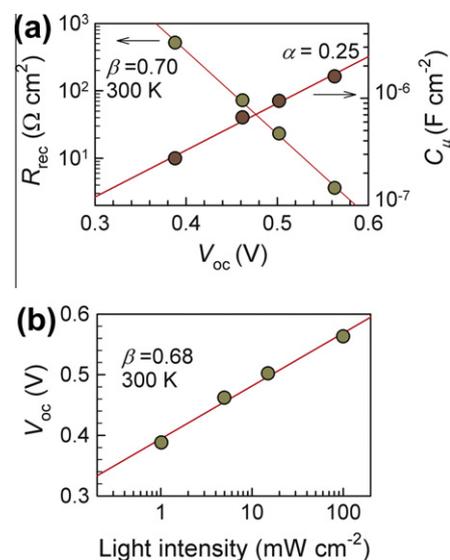
Fig. 1. (a) Recombination resistance of a P3HT:PCBM-based solar cell extracted from impedance spectroscopy exhibiting an exponential dependence on V_{oc} as $R_{rec} \propto \exp(-\beta qV_{oc}/k_BT)$, with $\beta = 0.70$, and chemical capacitance following $C_\mu \propto \exp(\alpha qV_{oc}/k_BT)$ with $\alpha = 0.25$. An estimation of the disorder degree results in $\sigma = k_BT/q\alpha \approx 100$ meV. (b) Open-circuit voltage dependence on light intensity following $V_{oc} \propto k_BT/\beta q \ln G$ with $\beta = 0.68$.

being L the active layer thickness. As an example of typical extracted parameters we show in Fig. 1 experimental results obtained for common P3HT:PCBM solar cells at room-temperature. From the capacitance dependence on V_{oc} it is feasible to estimate the charger carrier density by integration of $C_\mu(V_{oc})$ curve [26], which is a in fact representation of the carrier DOS as $C_\mu = q^2 g(V_{oc})$. We suggested that recombination losses restrict the electronic site occupancy to the tail of the DOS because surviving photogenerated carriers thermalize into deeper lying states. Gaussian [26] as well as exponential [28] DOS have been proposed accounting for the electron states distribution, although it is hard distinguishing between both in practical experiments because usual illumination intensities are only able to reach low-occupancy conditions (10^{15}–10^{18} cm^{-3}) [28]. Dependences of both resistance and capacitance on V_{oc} exhibit exponential laws as $C_\mu \propto \exp(\alpha q V_{oc}/k_B T)$, and $R_{rec} \propto \exp(-\beta q V_{oc}/k_B T)$ with $\alpha = 0.25$, and $\beta = 0.70$, respectively (Fig. 1a). Since measurements are performed at room-temperature one can evaluate the characteristic energy of the DOS that results in $\sigma = k_B T/q\alpha \approx 100$ meV, which gives an estimation for the energy broadening (disorder degree), in agreement with usually reported values [20,21].

From Eq. (4) and the experimentally observed exponential dependence of the recombination resistance on V_{oc}, one recovers Eq. (2). Since solar cells are kept in open-circuit conditions at which the kinetic balance between photogeneration and charge recombination holds, it is readily implied that $V_{oc} \propto k_B T/\beta q \ln j_{rec} \propto k_B T/\beta q \ln G$. This last proportionality relations occur because $j_{rec}(V_{oc}) = j_{ph} \propto G$, in accordance to the electronic reciprocity relationship (local carrier density and outer voltage determine each other) [25,29]. For solar cells having a performance severely limited by carrier transport effects the electronic reciprocity might fails, but it has been demonstrated that this is not the case of P3HT:PCBM-based devices [23]. Consequently the parameter β in the recombination resistance–dependence on V_{oc} equals the slope $k_B T/\beta q$ in the relation $V_{oc} \propto \ln G$. A direct measurement of V_{oc} dependence on illumination intensity shown in Fig. 1b allows corroborating such expectation. It is observed that the slope in the relation $V_{oc} \propto \ln G$ is larger than $k_B T/q$ with $\beta = 0.68$. We highlight at this point that the deviation from the simpler Boltzmann regime can be observed either from impedance spectroscopy analysis or through the irradiation intensity variation of the photovoltage.

In our previous papers energy disorder was identified as being the cause of the open-circuit voltage offset with respect to the effective band gap [3,30]. In those works basic phenomenology (V_{oc} reduction with respect to the effective gap, temperature coefficient, and light-dependence of the photovotage) was addressed. E_g was interpreted as the energy distance between distribution centers ($E_g = 1.5$ eV in this study). This yields an energy offset of ≈ 1.1 eV if the onset of fullerene reduction (polymer oxidation) peak from cyclic voltammetry is used to define the effective band-gap. We assumed Gaussian DOS distributions of donor HOMO and acceptor LUMO manifolds with width σ_n for the acceptor fullerene, and σ_p for the donor polymer [31].

Recombination is described by a charge-transfer between an occupied electron state of the LUMO manifold and an unoccupied hole state of the HOMO distribution [32]. In our approach all carriers participate into the recombination process no matter where the occupied energy level is. We adopted the Marcus model approach [33], which involves a reorganization energy λ. In addition the simulation imposes $R(E_{Fn}, E_{Fp}) = G$, and the electroneutrality constraint given by $n(E_{Fn}) = p(E_{Fp})$. The Fermi level positions can be evaluated by requiring the system of equations to satisfy the previously mentioned conditions: first photogeneration rate must be balanced by the recombination rate, and the absorber layer should be space-charge free. Simulation also assumes perfectly selective ohmic contacts [3,30].
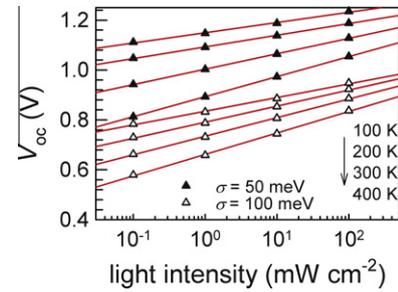
Fig. 2. Open-circuit voltage resulting from model simulations as a function of light intensity, for different temperatures and disorder degrees. Parameters used in the simulation: $E_g = E_{LUMO}(A) - E_{HOMO}(D) = 1.5$ eV, $N_{LUMO} = N_{HOMO} = 10^{20}$ cm^{-3}, recombination coefficient $k = 10^{-13}$ cm^3 s^{-1}, $\lambda = 1$ eV, and $G = 7.5 \times 10^{16}$/L cm^3 s^{-1} (layer thickness $L = 100$ nm) corresponds to $I = 100$ mW cm^{-2}. Other parameters marked in each curve, and $\sigma_n = \sigma_p$. A linear response is observed as $V_{oc} \propto k_B T/\beta q \ln G$.
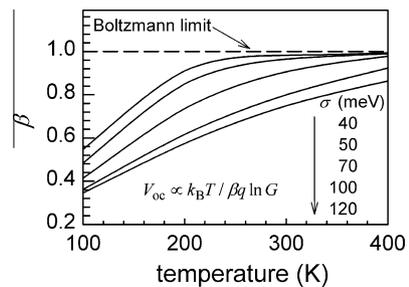
Fig. 3. Variation of β-parameter calculated from the slopes $k_B T/\beta q$ in Fig. 2 as a function of temperature, for different disorder degree σ.

Fig. 2 shows calculations of the variation of V_{oc} with the logarithm of the light intensity for different degrees of disorder, using a representative set of simulation parameters [3,30]. We note that the expected relation $V_{oc} \propto \ln G$ is always observed regardless the temperature and the disorder degree. In Fig. 3 the slope is plotted as a function of the temperature in terms of the β parameter in $k_B T/\beta q$ that results within $0 < \beta \leqslant 1$. One can observe that only for weak disorder ($\sigma < 50$ meV) $\beta \approx 1$ for temperatures in excess of 200 K. For more physically realistic disorder ($\sigma = 50$ meV) a clear transition is exhibited between a nearly Boltzmann regime at high temperatures ($T > 250$ K), and a response with larger slope values $\beta < 1$. Higher disorder degrees produce in all cases strong deviations from the ideal Boltzmann statistics. In order to explore whether the slope change (represented by the β parameter) is actually produced by the energy disorder, and not to the variations of the recombination rate on energy as implied by the Marcus rate approach [3,30], another set of simulations are carried out which includes the energy-independent recombination rate as $R = knp$ with a constant k. Similar trends are encountered (not shown) which reinforce the idea it is actually disorder that produces the observed deviations from the ideal Boltzmann behavior.

The reason behind the variation of the slope $k_B T/\beta q$ in the relation $V_{oc} \propto \ln G$ is connected with the concept of the charge carrier equilibration energy, usually employed in studies of carrier transport in disordered media [31]. One can alternatively understand it in terms of the so-called thermodynamic factor which allows calculating the deviation from the Boltzmann statistics [34,35]. In steady-state conditions, low disorder, high-temperature and low occupancy ($n/N_{LUMO} < 10^{-2}$), the photogenerated carriers, which are initially distributed along DOS shape, thermalize into the Gaussian tail with an average, equilibration energy $\sigma_n^2/k_B T$ below E_{LUMO}. Such energy signals the mean energy level of the charge carriers and is located above the concentration-dependent Fermi
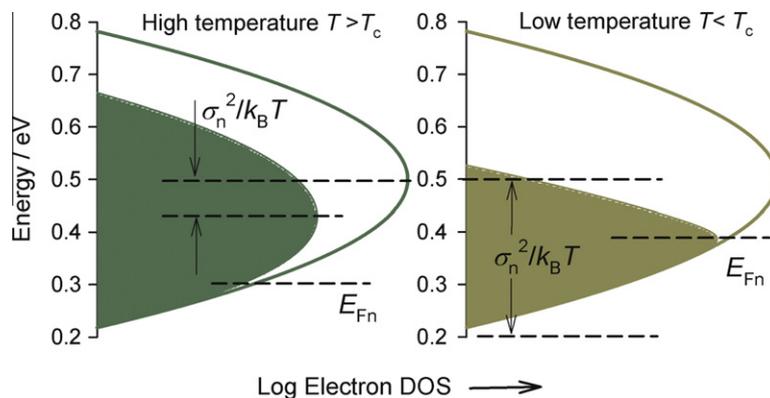
Fig. 4. Diagram of electron Gaussian density-of-states (solid line) and occupancy (filled) at high- and low-temperature respect to T_c. The position of electron Femi level and the equilibration energy $-\sigma_n^2/k_BT$ respect to the LUMO mean is indicated.
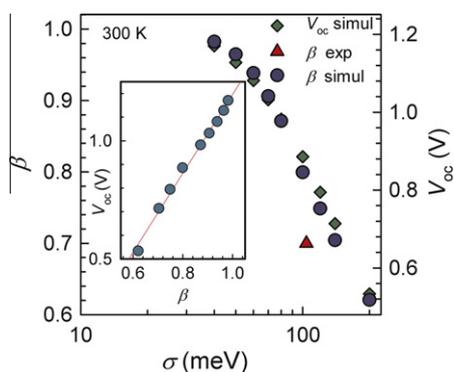
Fig. 5. Dependence of β-parameter and open-circuit voltage on disorder degree $\sigma = \sigma_n = \sigma_p$, at high-temperature (300 K) as derived from simulations in Fig. 2. A relationship of the type $\beta \propto \ln \sigma^{-1}$ is observed. Triangle indicates experimental values of β and σ extracted from impedance measurements in Fig. 1. In the inset: linear correlation as $V_{oc} \propto \beta$.

level, i.e. $E_{Fn} < \sigma_n^2/k_BT$ (see Fig. 4) [31]. Similarly for holes one can define σ_p^2/k_BT above E_{HOMO}. Because of the lower location of the Fermi level in case of low occupancy, the equilibration energy σ^2/k_BT establishes an upper limit to the achievable photovoltage. Under these conditions carriers follow the Boltzmann statistics and a slope equal to k_BT/q is expected. In this particular case is even possible to give an analytical expression for V_{oc}. A straightforward calculation allows determining the Fermi level positions [36] from which [30].

$$qV_{oc} = E_g - \frac{\sigma_n^2 + \sigma_p^2}{2k_BT} - k_BT \ln\left(\frac{N_{LUMO}N_{HOMO}}{np}\right) \quad (5)$$

This last expression contains the term related to the electron and hole equilibration energies as discussed above. Note here that the second summand is not present in the Fermi level splitting calculation given in Eq. (1), and it can be interpreted as a reduction of the effective bandgap $E_g' = E_g - (\sigma_n^2 + \sigma_p^2)/2k_BT$.

For larger disorder and low-temperature the equilibration energy is placed deep into the bandgap. For disorder values around 50 meV there exists a critical temperature $T_c \approx 250$ K at which $E_{Fn} = -\sigma_n^2/k_BT$ respect to the LUMO mean and $E_{Fp} = \sigma_p^2/k_BT$ respect to the HOMO mean. Above T_c occupancy obeys the Boltzmann approximation and consequently Eq. (5) could be applied. At lower temperatures $(T < T_c)$ the Fermi level is situated at energies higher than σ^2/k_BT, and coincides with the energy of maximum occupancy within the Gaussian DOS as depicted in Fig. 4. Under this regime the carrier no longer follows the Boltzmann approximation

(Eq. (5)) and consequently the slope in $V_{oc} \propto \ln G$ departs from k_BT/q. Strong disorder ($\sigma > 50$ meV) produces deviations ($\beta < 1$ as observed in Fig. 3) within the whole temperature range explored. This response appears as a distinctive feature of organic disordered compounds related to the Gaussian DOS occupancy. The two extreme regimes (Boltzmann for high-temperature and $\sigma \leqslant 50$ meV, and non-ideal for larger disorder) are drawn in the energy scheme of Fig. 4.

Because solar cells function around room-temperature it is shown in Fig. 5 the variation of β as a function of the disorder degree. As observed β is extremely sensitive to small changes of σ within the range of 50–100 meV, following a relationship as $\beta \propto \ln \sigma^{-1}$. We remark that parameters extracted from the impedance analysis shown in Fig. 1 correlate well with the predicted relationship between energy disorder and β-recombination model in Eq. (2), as confirmed by the location of the experimental point in Fig. 5. This implies that the recombination flux, and consequently the solar cell fill factor are highly influenced by the energy disorder degree, reducing the overall power-conversion efficiency. It is important to note here that the solar cell fill factor may have been also affected by deficient charge carrier transport, particularly for thicker active layer films.

As pointed out in previous works the energy distribution of electronic states (DOS) of both fullerene acceptor and polymer donor has turned to be a fundamental piece of knowledge for understanding solar cell performance [26,37]. Disorder was identified as a cause of reduction in V_{oc}, and this has been confirmed by alternative theoretical approaches more recently [4,35]. We highlight that reduction in V_{oc} follows exactly the same trend as that encountered for the variation of β with disorder (Fig. 5). One can infer therefore that $V_{oc} \propto \beta$ as observed in the inset of Fig. 5. For low disorder ($\sigma \approx 50$ meV) $\beta \approx 1$ at high temperature (300 K), a rough estimation of the total reduction in V_{oc} with respect to the effective bandgap can be calculating by using Eq. (5). The second summand amounts ~100 meV for $\sigma \approx 50$ meV, and additional drop in V_{oc} appears as a consequence of the partial DOS occupancy represented by the third summand in Eq. (5). Excess photogenerated charge carriers for usual illumination intensities around 1 sun, lies within $n \approx 10^{17}$–10^{18} cm^{-3} [28], so as to reduce further the Fermi level splitting in 350–250 meV, assuming $N_{LUMO} \approx N_{HOMO} \approx 10^{20}$ cm^{-3}. These rough estimations are in good agreement with the results of our simulation in Fig. 5.

When the Boltzmann approximation is no longer valid ($\beta < 1$) a dramatic drop in V_{oc} is derived. The experimentally observed correlation between the onset in fullerene reduction and polymer oxidation potentials, and the achieved V_{oc} at 1 sun irradiation intensity, $qV_{oc} \approx E_{LUMO}^{onset}(A) - E_{HOMO}^{onset}(D) - \Delta$ [38] (with $\Delta \approx 0.3$ eV) is

then understood in terms of the DOS occupancy modulation. It is worth noting that for $\sigma \approx 100$ eV the usually reported value for photovoltage $V_{oc} \approx 0.6$ V for P3HT:PCBM-based solar cells is predicted as illustrated in Fig. 5.

3. Conclusions

In summary we have presented new evidences on the detrimental effect on solar cell performance of inherent energy disorder exhibited by organic materials. A connection is established between the disorder degree and the reduction in fill-factor (through the β-parameter entering the recombination current-dependence on voltage) on the one hand, and open-circuit voltage, on the other. A huge reduction in β and open-circuit voltage is predicted following a relationship as $V_{oc} \propto \beta \propto \ln \sigma^{-1}$. This implies that the recombination flux, and consequently the solar cell fill factor are highly influenced by the energy disorder degree, reducing the overall power-conversion efficiency.

Acknowledgements

References

[1] Green MA, Emery K, Hishikawa Y, Warta W, Dunlop ED. Solar cell efficiency tables (version 39). Prog Photovoltaics Res Appl 2012;20:12–20.

[2] Kirchartz T, Taretto K, Rau U. Efficiency limits of organic bulk heterojunction solar cells. The J Phys Chem C 2009;113:17958–66.

[3] Garcia-Belmonte G, Bisquert J. Open-circuit voltage limit caused by recombination through tail states in bulk heterojunction polymer-fullerene solar cells. Appl Phys Lett 2010;96:113301.

[4] Blakesley JC, Neher D. Relationship between energetic disorder and open-circuit voltage in bulk heterojunction organic solar cells. Phys Rev B 2011;84:075210.

[5] NP K, Garcia-Belmonte G, Kahn A, Bisquert J, Cahen D. Photovoltaic efficiency limits and material disorder. Energy Environ Sci 2012;5:6022–39.

[6] Kirchartz T, Pieters BE, Kirkpatrick J, Rau U, Nelson J. Recombination via tail states in polythiophene:fullerene solar cells. Phys Rev B 2011;83:115209.

[7] Etzold F, Howard IA, Mauer R, Meister M, Kim T-D, Lee K-S, et al. Ultrafast exciton dissociation followed by nongeminate charge recombination in PCDTBT:PCBM photovoltaic blends. J Am Chem Soc 2011;133:9469–79.

[8] Li L, Kwon JH, Jang J. Tail states recombination limit of the open circuit voltage in bulk heterojunction organic solar cells. Org Electron 2012;13:230–4.

[9] Giebink NC, Wiederrecht GP, Wasielewski MR, Forrest SR. Ideal diode equation for organic heterojunctions. I. Derivation and application.. Phys Rev B 2010;82:155305.

[10] Presselt M, Bärenklau M, Rösch R, Beenken WJD, Runge E, Shokhovets S, et al. Subbandgap absorption in polymer-fullerene solar cells. Appl Phys Lett 2010;97:253302.

[11] MacKenzie RCI, Kirchartz T, Dibb GFA, Nelson J. Modeling nongeminate recombination in P3HT:PCBM solar cells. The J Phys Chem C 2011;115:9806–13.

[12] Street RA. Localized state distribution and its effects on recombination in organic solar cells. Phys Rev B 2011;84:075208.

[13] Cheyns D, Poortmans J, Heremans P, Deibel C, Verlaak S, Rand BP, et al. Analytical model for the open-circuit voltage and its associated resistance in organic planar heterojunction solar cells. Phys Rev B 2008;77:165332.

[14] Cowan SR, Roy A, Heeger AJ. Recombination in polymer-fullerene bulk heterojunction solar cells. Phys Rev B 2010;82:245207.

[15] Koster LJA, Mihailetchi VD, Ramaker R, Blom PWM. Light intensity dependence of open-circuit voltage of polymer:fullerene solar cells. Appl Phys Lett 2005;86:123509.

[16] Mandoc MM, Kooisrta FB, Hummelen JC. Boer Bd, Blom PWM. Effect of traps on the performance of bulk heterojunction organic solar cells. Appl Phys Lett 2007;91:263505.

[17] Kuik M, Nicolai HT, Lenes M, Wetzelaer G-JAH, Lu M, Blom PWM. Determination of the trap-assisted recombination strength in polymer light emitting diodes. Appl Phys Lett 2011;98:093301.

[18] Tiedje T. Band tail recombination limit to the output voltage of amorphous silicon solar cells. Appl Phys Lett 1982;40:627–9.

[19] van Berkel C, Powell MJ, Franklin AR, French ID. Quality factor in a-Si:H nip and pin diodes. J Appl Phys 1993;73:5264.

[20] Hulea IN, Brom HB, Houtepen AJ, Vanmaekelbergh D, Kelly JJ, Meulenkamp EA. Wide energy-window view on the density of states and hole mobility in poly(p-phenylene vinylene). Phys Rev Lett 2004;93:166601.

[21] Bisquert J, Garcia-Belmonte G, García-Cañadas J. Effect of the Gaussian energy dispersion on the statistics of polarons and bipolarons in conducting polymers. J Chem Phys 2004;120:6726–33.

[22] Bisquert J, Garcia-Belmonte G. On voltage, photovoltage and photocurrent in bulk heterojunction organic solar cells. J Phys Chem Lett 2011;2:1950–64.

[23] Green MA. Solar cells: operating principles, technology, and system applications. New Jersey: Prentice Hall; 1981.

[24] Fabregat-Santiago F, Garcia-Belmonte G, Mora-Seró I, Bisquert J. Characterization of nanostructured hybrid and organic solar cells by impedance spectroscopy. Phys Chem Chem Phys 2011;13:9083–118.

[25] Boix PP, Guerrero A, Marchesi LF, Garcia-Belmonte G, Bisquert J. Current–voltage characteristics of bulk heterojunction organic solar cells: connection between light and dark curves. Adv Energy Mater 2011;1:1073–8.

[26] Garcia-Belmonte G, Boix PP, Bisquert J, Sessolo M, Bolink HJ. Simultaneous determination of carrier lifetime and electron density-of-states in P3HT:PCBM organic solar cells under illumination by impedance spectroscopy. Sol Energy Mater Sol Cells 2010;94:366–75.

[27] Bisquert J, Fabregat-Santiago F, Mora-Seró I, Garcia-Belmonte G, Giménez S. Electron lifetime in dye-sensitized solar cells: theory and interpretation of measurements. The J Phys Chem C 2009;113:17278–90.

[28] Maurano A, Hamilton R, Shuttle CG, Ballantyne AM, Nelson J, O'Regan B, et al. Recombination dynamics as a key determinant of open circuit voltage in organic bulk heterojunction solar cells: a comparison of four different donor polymers. Adv Mater 2010;22:4987–92.

[29] Donolato C. A reciprocity theorem for charge collection. Appl Phys Lett 1985;46:270–2.

[30] Garcia-Belmonte G. Temperature dependence of open-circuit voltage in organic solar cells from generation–recombination kinetic balance. Sol Energy Mater Sol Cells 2010;94:2166–9.

[31] Bässler H. Charge transport in disordered organic photoconductors. Phys Stat Sol (b) 1993;175:15–56.

[32] Kawatsu T, Coropceanu V, Ye A, Brédas JL. Quantum-chemical approach to electronic coupling: application to charge separation and charge recombination pathways in a model molecular donor-acceptor system for organic solar cells. The J Phys Chem C 2008;112:3429–33.

[33] Marcus RA. Electron transfer reactions in chemistry. Theory and experiment. Rev Mod Phys 1993;65:599–610.

[34] Roichman Y, Tessler N. Generalized Einstein relation for disordered semiconductors – implications for device performance. Appl Phys Lett 2002;80:1948–51.

[35] Manor A, Katz EA. Open-circuit voltage of organic photovoltaics: implications of the generalized Einstein relation for disordered semiconductors. Sol Energy Mater Sol Cells 2011;97:132–8.

[36] Baranovskii SD, Zvyagin IP, Cordes H, Yamashi S, Thomas P. Percolation approach to hopping transport in organic disordered solids. Phys Stat Sol (b) 2002;230:281–7.

[37] Garcia-Belmonte G, Boix PP, Bisquert J, Lenes M, Bolink HJ, La Rosa A, et al. Influence of the intermediate density-of-states occupancy on open-circuit voltage of bulk heterojunction solar cells with different fullerene acceptors. J Phys Chem Lett 2010;1:2566–71.

[38] Scharber M, Mühlbacher D, Koppe M, Denk P, Waldauf C, Heeger AJ, et al. Design rules for donor bulk-heterojunction solar cells-Towards 10% energy-conversion efficiency. Adv Mater 2006;18:789–94.